HTML ABSTRACT + LINKS

Microlens arrays with integrated pores as a multipattern photomask

Shu Yang[a)]
Department of Materials Science and Engineering, University of Pennsylvania, 3231 Walnut Street, Philadelphia, Pennsylvania 19104

Chaitanya K. Ullal and Edwin L. Thomas
Department of Materials Science and Engineering, Massachusetts Institute of Technology, 77 Massachusetts Avenue, Cambridge, Massachusetts 02139

Gang Chen and Joanna Aizenberg[b)]
Bell Laboratories, Lucent Technologies, 600 Mountain Avenue, Murray Hill, New Jersey 07974

(Received 17 January 2005; accepted 28 March 2005; published online 13 May 2005)

Photolithographic masks are key components in the fabrication process of patterned substrates for various applications. Different patterns generally require different photomasks, whose total cost is high for the multilevel fabrication of three-dimensional microstructures. We developed a photomask that combines two imaging elements—microlens arrays and clear windows—in one structure. Such structures can be produced using multibeam interference lithography. We demonstrate their application as multipattern photomasks; that is, by using the same photomask and simply adjusting (i) the illumination dose, (ii) the distance between the mask and the photoresist film, and (iii) the tone of photoresist, we are able to create a variety of different microscale patterns with controlled sizes, geometries, and symmetries that originate from the lenses, clear windows, or their combination. The experimental results agree well with the light field calculations. © *2005 American Institute of Physics*. [DOI: 10.1063/1.1926405]

Fabrication techniques for integrated circuits often rely on a patterned photoresist layer to protect underlying structures during etches and material depositions. Forming the desired structure on the photoresist layer involves passing light through a mask, which has a pattern of opaque chrome regions that block portions of the wave front of the light for each exposure.[1] In a production of an IC with a sequence of different two-dimensional (2D) vertical levels, wherein the structures and/or sizes vary with the fabrication level, a set of different chrome masks is required to form each of the different layers using conventional projection lithography. The masks for lithographic processes are expensive to fabricate and therefore, mask costs can be a significant portion of the total cost for the multilevel fabrication process of microstructures. Furthermore, it requires precision optical systems and steppers in both vertical and horizontal repositioning and registration.

An alternative route to multilevel structures is the gray scale lithography technique.[2] It uses a gray scale photomask that can modulate the light intensity according to the levels of gray and create multilevel features in a single exposure without the need for multiple photomasks and alignment steps. Typically the size transferred to the photoresist is the same as that in the mask. For micrometer periodicity, a reduction photolithography process[3] has been developed that uses gray scale masks in combination with microlens arrays. Microlenses are widely used in optical telecommunication devices that image, actuate, and couple light.[4] Arrays of stacked microlenses have been used as a lithographic method to replicate patterns from photomasks into a photoresist layer.[5] In the reduction lithography process, the projected light passes through the gray scale photomask, and then is focused by the microlens array to transfer, for example, macroscopic figures on the mask into multilevel microstructures in the photoresist on a planar substrate. While this approach allows controlling the size of the generated features, only one pattern determined by that on the original photomask can be created. In this article, we describe a photomask design that integrates an array of microlenses with a pattern of clear windows in one element, which can be used as a "multipattern" photolithographic mask to directly and efficiently produce variable microstructures of different sizes in a single exposure. This can be achieved by changing the dose, the development conditions, the spacing between the mask and the resist, and the tone of the resist without using a number of costly lithographic masks. We demonstrate, for example, the ability to generate a hexagonal pattern of variable sizes, a honeycomb structure, or a combination of the two that originate from the lenses or/and windows in the photomask.

The photomask design [Fig. 1(a)] was inspired by the structure of a biologically formed porous microlens array [Fig. 1(b)].[6] Brittlestars were shown to use this element as a tunable optical device: The lenses demonstrate remarkable focusing ability and guide light onto photosensitive nerve bundles, while a pore network surrounding the lenses is involved in the regulation of light intensity by pigment transport. We anticipated that the unique combination of both functional elements, *lenses* and *clear windows*, in one photomask would project different light patterns from lenses and pores, respectively, on a photoresist layer. Moreover, by varying the light dose and/or the distance between the porous microlens arrays and a photoresist, one could control the feature sizes and/or the symmetry of the produced pattern [Figs. 1(c) and 1(d)].

The microlens arrays with integrated pores were fabricated by three-beam interference lithography in a single exposure from a negative tone photoresist, SU8 (from Shell

[a)]Electronic mail: shuyang@seas.upenn.edu
[b)]Electronic mail: jaizenberg@lucent.com

 © 2005 American Institute of Physics
Downloaded 03 Jul 2005 to 192.11.226.120. Redistribution subject to AIP license or copyright, see http://apl.aip.org/apl/copyright.jsp

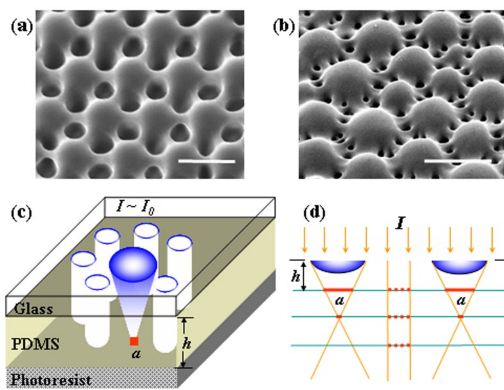

FIG. 1. (Color online) Biomimetic porous microlens array as a multipattern photomask. (a) Scanning electron micrograph (SEM) of a microlens array with integrated clear windows fabricated using multibeam interference lithography. Scale bar, 5 μm. (b) SEM of a biological porous microlens array formed by photosensitive brittlestars. Scale bar, 50 μm. (c) Schematic presentation of a photolithographic experiment with the porous microlens mask. (d) Schematic presentation of the photomask action at different distances from photoresist h and different light intensities I. For $I < I_{th}$, only features under the lenses are expected (shown as the bold lines). Their size a will depend on the distance from the focal point f. For $I > I_{th}$, the features under the lenses will be surrounded by the features originating from the windows (shown as the dotted lines). For $h > 2f$, only features under the windows are expected.

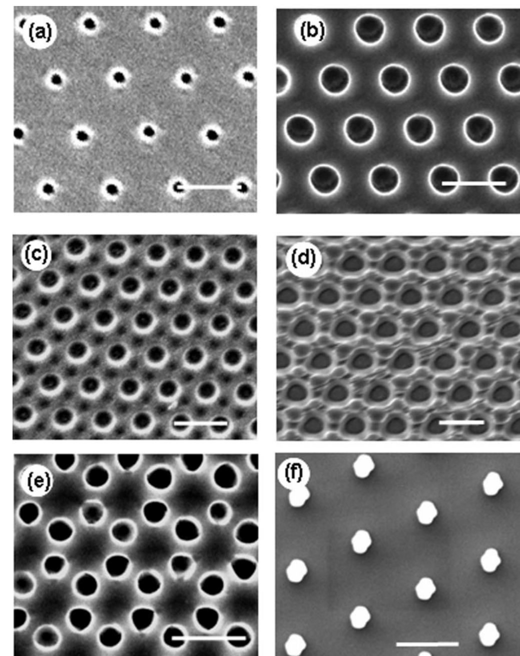

FIG. 2. Examples of photoresist patterns generated using the porous lens arrays as photolithographic masks. (a)–(e) from positive tone resists and (f) from a negative tone resist. (a) $I < I_{th}$, $h \sim f$; (b) $I < I_{th}$, $h < f$; (c) $I > I_{th}$, $h \sim f$; (d) $I > I_{th}$, $h < f$; (e) $I > I_{th}$, $h > 2f$; and (f) $I < I_{th}$, $h \sim f$.

Chemicals).[7] Multibeam interference lithography has been shown as a fast, simple, and versatile approach to create 2D and 3D periodic dots or porous microstructures defect free over a large area.[7–11] In our experiment, we fine tuned the beam polarization, such that the periodic variation in the intensity of light in the interference pattern introduced a contour of a lens in the highly exposed regions, while the unexposed or very weakly exposed areas formed pores after development.[7] We can control the lens size (diameter of 1.5 to 4.5 μm, height of $\sim$200 nm to 1.0 μm) and shape, as well as the symmetry and connectivity of the pattern by adjusting the beam wave vectors and their polarizations, while the pore size and porosity are determined by the laser intensity and exposure time (porosity of about 10% to 80%). An exemplary structure comprising a hexagonal array of lenses and pores is shown in Fig. 1(a). The detailed interference lithography procedure can be found in the literature.[7] The lenses measured in an atomic force microscope (AFM) appeared to be semispherical, with a height of 820 nm and a periodicity of 5 μm. Figure 1(c) provides a schematic illustration of a lithographic experiment, in which a photoresist film was illuminated through thus fabricated photomask.

We first investigated the fabrication of microstructures in a positive-tone photoresist through the porous microlens arrays. A 1-μm-thick film of AZ5209 (from Clariant International Ltd.) was spun on a glass substrate, followed by casting a film of poly(dimethylsiloxane) (PDMS) on top of the resist as a transparent spacer. The mask attached to a glass substrate was then placed directly on the PDMS spacer for conformal contact. The wavelength of exposure light was 365 nm. When the illumination dose is fixed slightly below the sensitivity threshold of the photoresist (I_{th}), no pattern is expected to originate from the light passing through the clear windows, while the focusing activity of the lenses enhances the light field near focus to surpass the resist threshold intensity. Indeed, for $I < I_{th}$, features in photoresist were selectively generated under the lenses, showing hexagonally packed holes [Figs. 2(a) and 2(b)] that closely matched the microlens array in the mask [see Fig. 1(a)]. The size of the features in the resist layer a can be effectively controlled by placing transparent PDMS spacers with different thickness h between the lens and the resist film. The diameter of the generated holes in the photoresist gradually changed from $\sim$3 μm to a minimum value of $\sim$700 nm when h was increased from 1 to 8 μm.[11] The minimum dose to realize patterns under the lenses (i.e., holes near the focal point at a distance of $\sim$8 μm) was $\sim$2 mJ/cm^2, while normally the dose of $>$40 mJ/cm^2 is needed to produce a good feature in the photoresist using a conventional chrome mask.

For the illumination dose set above the lithographic threshold intensity of photoresist ($I > I_{th}$), we generated patterns originated from both the lenses and the windows [Figs. 2(c) and 2(d)]. The relative sizes of the features formed from the lenses and pores are controlled by the distance between the lens structure and the resist film. When $I > I_{th}$ and $h > 2f$, we observed a honeycomb structure originated from the light coming through the pores only [Fig. 2(e)]. The microscale honeycomb structures are of interest as 2D photonic crystals with a large band gap.

A variety of microstructures can also be formed when using a negative tone resist (e.g., SU8). We observed hexagonally packed dots that corresponded to the hexagonal lens array in the mask, when $I < I_{th}$ [Fig. 2(f)]. By adjusting the illumination dose above I_{th} and the distance between SU8 and the mask, a pattern of a hexagonal array of dots of one size surrounded by six dots of a different size could be formed. The structures generated in negative resists had a lenslike profile, while their size was reduced compared to the size of the original lenses in the photomask. The contour of the newly formed lenses can be further modulated by the nonlinear response of a chosen negative resist system to the dose, its polymerizability and the solubility contrast during resist development.

Downloaded 03 Jul 2005 to 192.11.226.120. Redistribution subject to AIP license or copyright, see http://apl.aip.org/apl/copyright.jsp

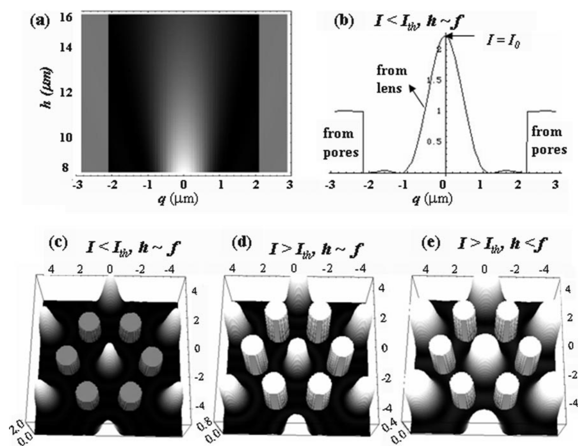

FIG. 3. Calculated light field profiles generated by the porous microlens array in a lithographic experiment at different illumination doses and distances. (a) Light field distribution from a single lens for $h=f$ to $h=2f$; (b) Cross section of the field produced by the lens vs that from the pores for $I<I_{\rm th}$, $h\sim f$; (c)–(e) 3D light intensity profiles generated for $I<I_{\rm th}$, $h\sim f$ (c); $I>I_{\rm th}$, $h\sim f$ (d), and $I>I_{\rm th}$, $h<f$ (e).

To quantitatively study the lithographic process with the porous lens array photomask, we simulated the light intensity distribution from both pores and lenses using simple Fourier optics (Fig. 3).[12] The lens was assumed to be diffraction limited at its focus and the light field to be an airy ring given by the following equation:

$$I = I_0[2J_1(krq/h)/(krq/h)]^2, \quad (1)$$

where I_0 is the peak intensity at that plane, J_1 is the first Bessel function (commonly used in systems with cylindrical symmetry, such as lenses), k is the modulus of the wave vector of the light, r is the radius of the lens, q is the radial distance from the optical axis, and h is the distance along the optical axis, i.e., the distance between the lens array and the photoresist. Since the light falling on the lens has to be conserved, we normalized the value of I_0 against the intensity of light falling on the lens. Based on the experimental data, the focal length of the lens f was set at 8 μm, and the diameters of the lenses and pores were assumed 3 and 1.5 μm, respectively.

Figure 3(a) shows the calculated light field of a lens from $h=f$ to $h=2f$. The light passing through the lens is focused with the highest intensity at $h=f$ and $q=0$. The peak intensity is I_0. The pores were assumed to generate a cylindrical light profile, whose peak intensity is determined by the illumination dose [Fig. 3(b)]. We can estimate the size of the feature in the focal point by calculation. If we look at the threshold intensity from pores in Fig. 2(b) as the cut-off intensity and find the value on the x axis for the lens, we obtain the radius of $\sim$0.4 μm (0.8 μm in diameter). This value is very close to our experimental data (0.7 μm in diameter), considering that we did not take into account the possible inhomogeneity of the lens shape due to the Gaussian distribution of the light intensity across the film in the three-beam interference experiment. The calculated 3D profiles of the light field generated by the photomask for $I<I_{\rm th}$, $I>I_{\rm th}$ and at different h are shown in Figs. 3(c)–3(e). The light field calculations agree well with the corresponding experimental results shown in Fig. 2.

The effect of the junctions between the lenses was not included into calculations due to the following reasons. The radius of the curvature of the junction and therefore their focal distance f_j are small compared to the corresponding lens value f. As a result, the light produced by the junctions at the distances of interest ($\geqslant f$) is diffuse and its contribution to the final pattern formation is negligible. The fact that the calculation and experiment agree well suggests that the model we propose is indeed a good approximation of the real structure, and captures all significant features of the photomask that contribute to the generated pattern size and symmetry.

In conclusion, we have developed a photomask design that integrates two types of imaging elements (clear windows and lenses) into one structure. We demonstrated that this structure could be applied as a *multipattern* photolithographic mask capable of producing structures with variable sizes *and* patterns, a feature which is not achievable using traditional, gray scale, or reduction lithography approaches. In particular, different patterns with controlled sizes, geometry, topography and symmetry can be formed using a single mask, by choosing (i) the illumination dose below or above the lithographic threshold, and therefore the light intensity reaching the photoresist film through the lenses versus the pores; (ii) the distance between the lens array and the photoresist, to selectively generate patterns from the lenses and/or the pores; and (iii) the tone of the photoresist to obtain either holes or dots in positive or negative tone resists, respectively. This lithographic method may represent an attractive approach for fast and mass production of (sub)micron, periodic structures at a low cost.

This work is supported in part by the UPenn start-up fund, the University Research Foundation, the DuPont Science and Engineering Award, and the National Science Foundation (BES-0438004). The authors gratefully acknowledge their respective support from Skirkanich term chair (S.Y.), the U.S. Air Force Defense University Research Initiative on Nanotechnology in conjunction with the University of Buffalo (C.K.U.), and the Institute for Soldier Nanotechnologies of the U.S. Army Research Office (E.L.T.). The authors thank Chada Ruengruglikit and Qingrong Huang (Rutgers University) for their help with the AFM measurements, and C.K.U. thanks J. Walish for assistance with the calculations.

[1] L. F. Thompson, C. G. Willson, and M. J. Bowden, *Introduction to Microlithography*, 2nd ed. (American Chemical Society, Washington, DC, 1994).
[2] E. B. Kley, Microelectron. Eng. **34**, 261 (1997).
[3] H. K. Wu, T. W. Odom, and G. M. Whitesides, Anal. Chem. **74**, 3267 (2002); J. Am. Chem. Soc. **124**, 7288 (2002).
[4] D. Daly and M. C. Hutley, Pure Appl. Opt. **6**, U3 (1997).
[5] R. Völkel, H. P. Herzig, P. Nussbaum, R. Dandliker, and W. B. Hugle, Opt. Eng. **35**, 3323 (1996).
[6] J. Aizenberg, A. Tkachenko, S. Weiner, L. Addadi, and G. Hendler, Nature (London) **412**, 819 (2001); J. Aizenberg and G. Hendler, J. Mater. Chem. **14**, 2066 (2004).
[7] S. Yang, G. Chen, M. Megens, C. K. Ullal, Y.-J. Han, R. Rapaport, E. L. Thomas, and J. Aizenberg, Adv. Mater. (Weinheim, Ger.) **17**, 435 (2005).
[8] V. Berger, O. GauthierLafaye, and E. Costard, J. Appl. Phys. **82**, 60 (1997).
[9] M. Campbell, D. N. Sharp, M. T. Harrison, R. G. Denning, and A. J. Turberfield, Nature (London) **404**, 53 (2000).
[10] S. Yang, M. Megens, J. Aizenberg, P. Wiltzius, P. M. Chaikin, and W. B. Russel, Chem. Mater. **14**, 2831 (2002).
[11] Y. V. Miklyaev, D. C. Meisel, A. Blanco, G. von Freymann, K. Busch, W. Koch, C. Enkrich, M. Deubel, and M. Wegener, Appl. Phys. Lett. **82**, 1284 (2003).
[12] Eugene Hecht, *Optics*, 2nd ed. (Addison Wesley, Reading, MA, 1987).

Downloaded 03 Jul 2005 to 192.11.226.120. Redistribution subject to AIP license or copyright, see http://apl.aip.org/apl/copyright.jsp